Dynamin 2 mediates fluid-phase micropinocytosis in epithelial cells

Hong Cao, Jing Chen, Muyiwa Awoniyi, John R. Henley and Mark A. McNiven*

Mayo Clinic, Department of Biochemistry and Molecular Biology and the Miles and Shirley Fiterman Center for Digestive Diseases, Rochester, MN 55905, USA

*Author for correspondence (e-mail: mcniven.mark@mayo.edu)

Accepted 17 September 2007
Journal of Cell Science 120, 4167-4177 Published by The Company of Biologists 2007
doi:10.1242/jcs.010686

Summary

It is well-known that dynamin 2 (Dyn2) participates in clathrin- and caveolae-mediated endocytosis; however, the role of Dyn2 in coat-independent endocytic processes remains controversial. Here we demonstrate a role for specific spliced variants of Dyn2 in the micropinocytosis of fluid in epithelial cells, independent of coat-mediated endocytic pathways. A general inhibition of Dyn2 was first performed using either microinjection of anti-dynamin antibodies or *Dyn2*-siRNA treatment. Both of these methods resulted in reduced uptake of transferrin, a marker for clathrin-mediated endocytosis, and, under unstimulated conditions, reduced the uptake of the fluid-phase markers dextran and horseradish peroxidase (HRP). By contrast, cells treated similarly but stimulated with serum or EGF internalized substantial amounts of dextran or HRP, indicating that Dyn2 is not required for stimulated fluid uptake via macropinocytosis. We next tested whether a specific spliced variant might selectively affect fluid-phase endocytosis. Mutation of specific Dyn2 spliced variants resulted in a differential attenuation of transferrin and dextran internalization. Furthermore, the reduction in fluid uptake in *Dyn2*-siRNA-treated cells was only rescued upon re-expression of select spliced variants. These findings suggest that Dyn2 function is required for the coat-independent internalization of fluid through endocytic pathways distinct from macropinocytosis and, in addition, implicate different Dyn2 spliced variants in specific endocytic functions.

Supplementary material available online at
http://jcs.biologists.org/cgi/content/full/120/23/4167/DC1

Key words: Clathrin-independent, Dynamin 2, Fluid-phase endocytosis, Macropinocytosis, Micropinocytosis, Spliced variants

Introduction

Clathrin-independent fluid-phase endocytosis is a ubiquitous yet enigmatic internalization process used by cells to sample the external environment, internalize specific surface receptors and bacterial toxins, and sequester glycosylphosphatidylinositol (GPI)-anchored proteins (Conner and Schmid, 2003; Johannes and Lamaze, 2002; Kirkham and Parton, 2005; Mayor and Pagano, 2007; Nichols and Lippincott-Schwartz, 2001). Recent studies have suggested that what was once considered a single pathway is actually a collection of distinct non-clathrin-mediated pathways that appear to differ in their dependence on specific lipids, on non-clathrin coat proteins and on small regulatory GTPases, such as Cdc42, Rho and Arf6. Despite the importance of these pathways, remarkably little is known about how they might differentially sequester receptor-ligand cargo or form nascent uncoated vesicles. For example, conventional dynamin has been shown to mediate the formation of coated vesicles (Hinshaw, 2000; McNiven et al., 2000; Slepnev and De Camilli, 2000); however, the role of dynamin in the various coat-independent endocytic pathways is unclear (Conner and Schmid, 2003; Mayor and Pagano, 2007; Nichols and Lippincott-Schwartz, 2001).

Three distinct dynamin genes are expressed in mammalian cells: *Dyn1* appears to be neuronal specific, *Dyn2* might be ubiquitous and has been observed in all tissues examined to date, and *Dyn3* is expressed in a limited number of tissues, including the brain, testis, lung and heart. In addition to the three different dynamin isoforms, each of these isoforms exhibits a substantial level of alternative splicing (Cao et al., 1998; Urrutia et al., 1997), not unlike the single dynamin gene (known as *shibire*) expressed in flies (Staples and Ramaswami, 1999). Thus, in mammalian cells, many different dynamin protein products might exist that could target to distinct cellular locations and mediate diverse functions, from vesicle formation to cytoskeletal dynamics (Hinshaw, 2000; Kruchten and McNiven, 2006; McNiven et al., 2000; Orth and McNiven, 2003; Schafer, 2004).

Although it is well accepted that dynamin participates in clathrin- and caveolae-mediated endocytosis, the role of dynamin in coat-independent fluid-phase endocytosis has been more controversial. Early on, analysis of endocytosis in *shibire* temperature-sensitive (*shibire^{ts}*) mutant flies at the restrictive temperature using electron microscopy revealed a significant block in the uptake of horseradish peroxidase (HRP) (Kosaka and Ikeda, 1983), suggesting that dynamin participates in various fluid-phase endocytic pathways. However, in a more recent study, fluid-phase endocytosis appeared to be normal in temperature-shifted primary hemocytes isolated from *shibire^{ts}* flies (Guha et al., 2003). Similarly, cultured mammalian epithelial cells (COS7, HeLa) expressing dominant-negative Dyn1 or Dyn2 GTPase mutants have also been observed to internalize fluid-phase markers (Altschuler et al., 1998; Damke et al., 1994; Herskovits et al., 1993). Moreover, although HRP uptake was initially decreased in HeLa cells expressing a temperature-sensitive Dyn1 mutant, following prolonged

incubation at the restrictive temperature levels of internalized HRP recovered to that of control cells, or more (Damke et al., 1995), suggesting that inhibition of Dyn1 could induce a compensatory endocytic pathway for fluid uptake. Indeed, a Cdc42-dependent, Dyn2-independent pathway used to internalize GPI-linked proteins and thought to be a main mechanism of fluid-phase endocytosis in many cell types, both epithelial cells and fibroblasts, has been identified (Kirkham et al., 2005; Sabharanjak et al., 2002). In addition, dextran uptake in COS7 cells and mouse embryonic fibroblasts (MEFs) was recently observed to be independent of Dyn2 function but rather mediated by carboxy-terminal binding protein 3/brefeldin A-ribosylated substrate (CtBP3/BARS) (Bonazzi et al., 2005). Interestingly, MEFs from BARS knockout mice still internalize dextran and, moreover, fluid uptake under these conditions becomes sensitive to Dyn2 inhibition (Bonazzi et al., 2005). Finally, similar to the initial ~50% reduction in HRP uptake observed in Dyn1 temperature-sensitive-mutant-expressing cells at the restrictive temperature (Damke et al., 1995), BSC1 cells treated with the dynamin small-molecule inhibitor dynasore were found to exhibit an ~60% reduction in HRP uptake (Macia et al., 2006).

The observations described above used a variety of cell types, assays for assessing fluid uptake and methods of inhibiting dynamin function, including the use of mutants of different dynamin isoforms and spliced variants. In the current study, we implemented several approaches and a variety of cultured epithelial cell types in an attempt to perform a comprehensive analysis of the role of Dyn2 in fluid-phase endocytosis. The Dyn2 isoform and the four known alternative spliced variants, termed Dyn2(aa), Dyn2(ab), Dyn2(ba) and Dyn2(bb) (Cao et al., 1998; Sontag et al., 1994), were analyzed because Dyn2 is the only known conventional dynamin expressed in epithelial cells. In an earlier study, we defined distinct differences in the cytoplasmic distribution of some of the dynamin isoforms and spliced variants (Cao et al., 1998). It now seems likely that this diversity in spliced-variant distribution, and thus potentially in the cellular site of action, could account for some of the differences observed when testing the effects of inhibiting dynamin function on fluid-phase endocytosis. We first inhibited all Dyn2 forms either through microinjection of inhibitory anti-dynamin antibodies or by small interfering RNA (siRNA)-mediated reduction of Dyn2 protein levels. Subsequently, the uptake of fluorescently-labeled dextran was quantitated using a morphological method based on fluorescence intensity measurements and a biochemical enzymatic assay was used to quantitate HRP uptake (siRNA-treated cells only). Both antibody microinjection and siRNA treatment resulted in a significant inhibition in the uptake of transferrin (a marker for clathrin-mediated endocytosis used as a control) and, under low serum conditions (0.2% FBS), the fluid-phase markers dextran and HRP. By contrast, internalization of fluid via macropinocytosis following stimulation with high levels of serum (10% FBS) or epidermal growth factor (EGF; 30 ng/ml) appeared to be unaffected. To test whether a specific Dyn2 spliced variant might participate in fluid-phase endocytosis, we examined the distribution of wild-type and mutant versions of the four Dyn2 spliced variants and tested for a differential contribution to fluid-phase endocytosis. Interestingly, dominant-negative GTPase mutants of two specific Dyn2 spliced variants, Dyn2(ba) and Dyn2(bb), attenuated dextran uptake when compared with cells expressing wild-type Dyn2. Moreover, re-expression of either of these two spliced variants in *Dyn2*-siRNA-treated cells rescued the inhibitory effects of Dyn2 depletion on dextran internalization under low serum conditions. These findings provide insights into the potential differential functions of the distinct Dyn2 spliced variants and also suggest an explanation for the contrasting observations from multiple groups on the contribution of Dyn2 to fluid-phase endocytosis.

Results

Inhibition of Dyn2 function by antibody microinjection or *Dyn2*-siRNA treatment blocks fluid-phase endocytosis of dextran

The role of any Dyn2 spliced variant in fluid-phase endocytosis is controversial. Therefore, we first began testing whether Dyn2 participates in fluid uptake by attempting to inhibit the function of all Dyn2 spliced variants through microinjection of affinity-purified anti-dynamin antibodies into a variety of different epithelial cell lines (Clone 9, BNL CL.2, MDCK and HeLa). Following microinjection, cells were assayed for their ability to internalize fluorescently labeled transferrin (clathrin-mediated endocytosis), cholera toxin B (caveolae-mediated endocytosis) or dextran (fluid-phase endocytosis). The inhibitory antibodies used here were generated either against a peptide covering a highly conserved region immediately downstream of the N-terminal GTPase domain that is present in all of the conventional dynamins (MC65) or against a peptide encompassing a region in the C-terminal 'tail' of the Dyn2 isoform (anti-Dyn2), and have previously been shown to inhibit clathrin- and caveolae-mediated endocytosis (Henley et al., 1998). Injection buffer, anti-kinesin antibodies (MC44), anti-caveolin-1 antibodies or heat-inactivated anti-Dyn2 antibodies were microinjected as controls (Fig. 1A-D and supplementary material Fig. S1). Blocking Dyn2 function in cultured rat hepatocytes (Clone 9 cells) by microinjection of either of the two inhibitory anti-dynamin antibodies reduced endocytosis of transferrin by ~60-70% when compared with control cells microinjected with buffer or anti-kinesin antibodies (Fig. 1E,G,I), supporting previous results (Henley et al., 1998). In addition, microinjection of the anti-dynamin antibodies also reduced the internalization of dextran to a similar extent (~50-60% reduction) (Fig. 1F,H,J). Mouse hepatocytes (BNL CL.2), MDCK and HeLa cells were assayed in a similar manner and also exhibited a marked reduction in transferrin and dextran internalization upon inhibition of Dyn2 function (supplementary material Fig. S1).

To provide a second method of testing the dependence of fluid-phase endocytosis on Dyn2 function, we next monitored dextran uptake in cells in which Dyn2 protein levels had been reduced through use of siRNA oligonucleotides. Clone 9 cells were either treated with a pooled mixture of siRNA duplexes targeting four different regions of rat *Dyn2* (supplementary material Fig. S2A) or were mock transfected, as a control, for 24-96 hours. Subsequently, cells were allowed to internalize transferrin (supplementary material Fig. S2) or dextran for 60 minutes in low (0.2% FBS) (Fig. 2A-B′) or high (10% FBS) (Fig. 2C,C′) serum medium. Although mock treatment had no effect on Dyn2 protein levels (Fig. 2A and supplementary material Fig. S2A,B) or on transferrin uptake (supplementary

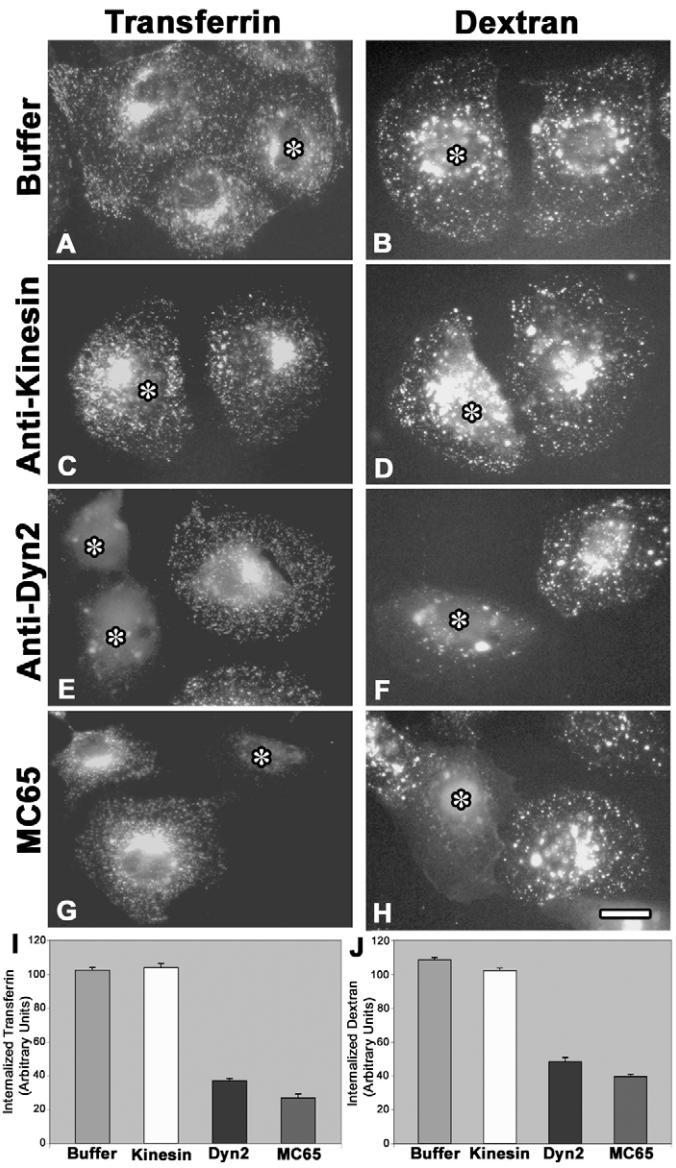

Fig. 1. Microinjection of purified anti-dynamin antibodies reduces fluid-phase endocytosis. (A-H) Fluorescence micrographs of Clone 9 cells microinjected with either a control solution (injection buffer or anti-kinesin antibodies) or affinity-purified peptide antibodies targeting Dyn2 and subsequently assayed for the internalization of fluorescently conjugated transferrin (A,C,E,G) or dextran (B,D,F,H). Control cells microinjected with either injection buffer alone (A,B) or purified inhibitory anti-kinesin antibodies (C,D) showed no reduction in the internalization of either fluorescently conjugated transferrin (A,C) or dextran (B,D). By contrast, microinjection of cells with 7.2-8.6 mg/ml of purified polyclonal anti-dynamin antibodies either specific for Dyn2 (E,F) or against a conserved region found in all conventional dynamins, MC65 (G,H), attenuated receptor-mediated and fluid-phase endocytosis. (*) Indicates an injected cell. (I,J) Quantitation of transferrin (I) and dextran (J) internalization in Clone 9 cells microinjected with either buffer alone, anti-kinesin antibodies or anti-dynamin antibodies based on measurement of fluorescence intensity units. Values obtained from microinjected cells were normalized to those of surrounding uninjected cells. Results represent the average ± s.d. of ⩾100 cells measured in each of two independent experiments. Bar, 10 μm.

material Fig. S2B′), treatment with either the pooled mixture of *Dyn2*-siRNA duplexes or *Dyn2*-siRNA duplex #2 reduced Dyn2 protein levels as well as transferrin uptake by ~70-80% (supplementary material Fig. S2A,C,D). In support of the microinjection experiments shown in Fig. 1, cells treated with *Dyn2* siRNA under low serum conditions also showed up to an ~70% reduction in fluid-phase endocytosis, as compared with mock-treated cells (Fig. 2A-B′,D).

Because fluid-phase markers such as dextran can enter cells not only through uncoated vesicles but also via caveolae- and clathrin-mediated endocytosis, which are both dynamin-dependent processes, it was important to measure the contribution of these endocytic pathways to fluid internalization. To assess the contribution of the caveolae- and clathrin-mediated pathways to fluid uptake, mouse hepatocytes (BNL CL.2) were treated with siRNA for 96 hours to reduce caveolin-1 or clathrin protein levels and then analyzed for protein reduction by immunofluorescent staining, and ligand and dextran internalization (supplementary material Fig. S3). Many cells showed a substantial reduction in caveolin-1 (supplementary material Fig. S3A-C) or clathrin (supplementary material Fig. S3E-G) staining following treatment with the corresponding siRNA, and this correlated with a reduced capacity to internalize either cholera toxin B (~75% reduction; supplementary material Fig. S3A′,D) or transferrin (~60% reduction; supplementary material Fig. S3E′,H), respectively. Despite the substantial impairment of these internalization processes, we observed no measurable effect on fluid-phase endocytosis in these cells (caveolin-1 siRNA, supplementary material Fig. S3B′-D′; clathrin siRNA, supplementary material Fig. S3F′-H′), although we cannot rule out that disruption of one pathway has some stimulatory effects on dextran uptake by a compensatory pathway. Thus, the reduced internalization of dextran by Dyn2 disruption appears to mainly be due to a block of the micropinocytic pathway. However, because all endocytic pathways internalize some fluid, inhibition of the traditional clathrin and caveolar pathways might also make a minor contribution to this effect.

Interestingly, the reduction in dextran internalization in *Dyn2*-siRNA-treated cells was more modest when the assays were conducted in the presence of high serum (10% FBS) rather than low serum (0.2% FBS). Dextran uptake was reduced by ~60-67% in *Dyn2*-siRNA-treated cells assayed under low serum conditions, whereas similarly treated cells allowed to internalize dextran under high serum conditions exhibited an ~44-55% reduction in dextran uptake, as compared with mock-treated cells assayed under the respective serum conditions (Fig. 2D). A possible explanation for this difference is that a dynamin-independent endocytic process is upregulated by the presence of serum. Macropinocytosis, which is well-known to be stimulated by growth factors, is a specialized clathrin-independent component of fluid-phase endocytosis whereby cells internalize membrane and fluid into large (>200 nm) endocytic vesicles, which are present many times at cortical membrane ruffles (Nichols and Lippincott-Schwartz, 2001; Swanson and Watts, 1995). EGF is known to induce cortical ruffling and macropinocytosis in a variety of cell types. Thus, we tested the role of Dyn2 in macropinocytosis in both Clone 9 and HeLa cells by inhibiting Dyn2 function either through siRNA treatment or antibody microinjection and then analyzing the ability of these cells to

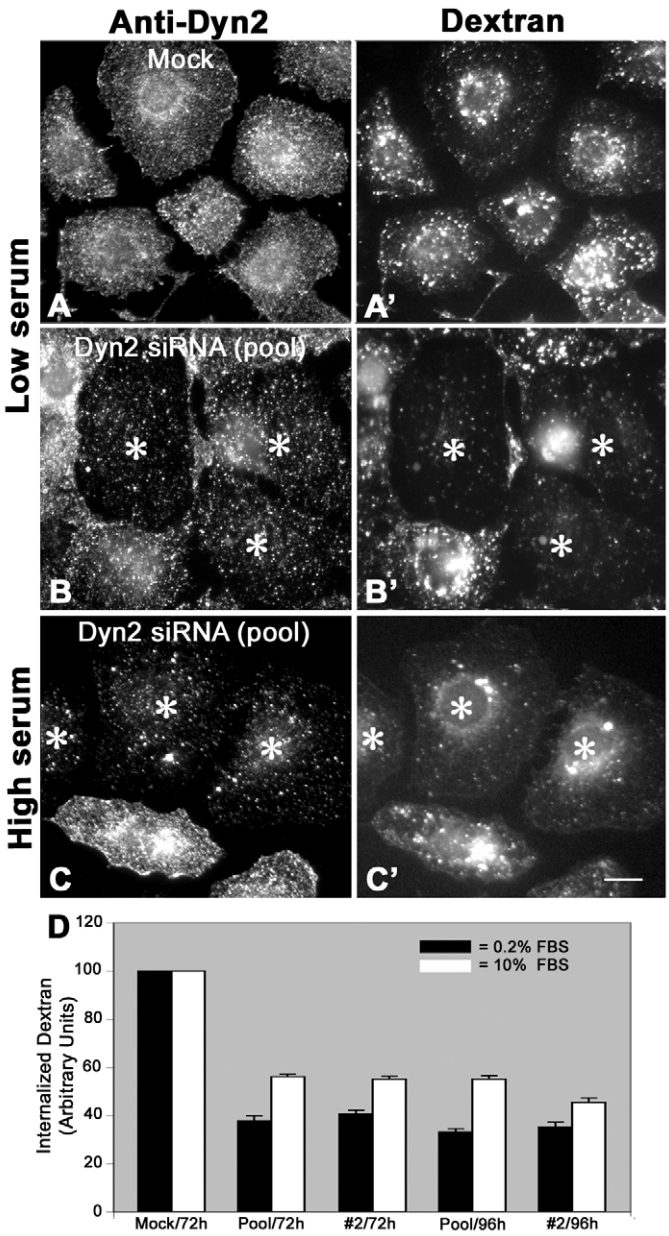

Fig. 2. Fluid-phase endocytosis is reduced in cells depleted of Dyn2 protein using siRNA treatment. (A-C′) Fluorescence micrographs of Clone 9 cells incubated with fluorescently conjugated dextran (A′,B′,C′) following either mock (A,A′) or *Dyn2* siRNA (B-C′) treatment. Dyn2 protein levels were analyzed by staining for Dyn2 using immunofluorescence (A,B,C). (A,A′) No effect on fluid-phase endocytosis was observed when cells treated with transfection reagent alone for 72 hours were allowed to internalize fluorescently conjugated dextran for 60 minutes in low serum medium (0.2% FBS). (B,B′) Cells transfected with a solution containing a pooled mixture of four distinct siRNA duplexes targeting *Dyn2* and assayed 72 hours later, as for cells in A,A′, showed a substantial reduction in Dyn2 staining (B) along with a marked reduction in the amount of dextran-positive cytoplasmic vesicles (B′). (C,C′) Treatment of cells as for B,B′ but in the presence of high serum medium (10% FBS): a more modest reduction in dextran internalization was observed than in low serum conditions. (*) Indicates a cell with reduced Dyn2 levels. (D) Quantitation of the amount of fluorescently conjugated dextran internalized by Clone 9 cells that had either been mock-treated for 72 hours, treated with a pooled mixture of *Dyn2* siRNA duplexes for 72 or 96 hours, or treated with *Dyn2* siRNA duplex #2 for either 72 or 96 hours, in the presence of low serum (black bars) or high serum (white bars) medium. Fluid-phase endocytosis was reduced in cells treated with either the pooled mixture of siRNA duplexes (Pool) or siRNA duplex #2 (#2), as compared with mock-treated cells, under both low serum (0.2% FBS) and high serum (10% FBS) conditions; however, the effect was more dramatic under lower serum conditions. Values obtained from siRNA-treated cells were normalized to those of mock-treated cells under similar serum conditions. Results represent the average ± s.d. of ⩾50 cells measured in each of three independent experiments. Bar, 10 μm.

internalize dextran under low serum conditions in the absence or presence of 30 ng/ml EGF. We found that dextran uptake was indeed attenuated to a lesser extent by Dyn2 depletion or anti-Dyn2 antibody microinjection in cells stimulated with EGF as compared with cells maintained in low serum (Fig. 3). Under low serum conditions in the absence of EGF, dextran uptake was reduced by ~60-70% in cells treated with *Dyn2* siRNA (Fig. 3A,B,E) and by ~55-70% in anti-Dyn2 antibody-injected cells (Fig. 3C,D,F) when compared with control cells. However, in cells stimulated with EGF, inhibition of Dyn2 function reduced dextran uptake by only ~25-30% (*Dyn2* siRNA; Fig. 3A′,B′,E) or ~20-35% (anti-Dyn2 antibody; Fig. 3C′,D′,F). Based on these similar findings using two distinct approaches – siRNA treatment and antibody microinjection – we conclude that macropinocytosis in the epithelial cells tested is Dyn2-independent and needs to be accounted for when measuring the role of any protein in fluid-phase endocytosis.

Importantly, these results also indicate that the methods used here to inhibit Dyn2 function do not randomly affect all endocytic processes.

As an additional morphological method and as a biochemical approach to monitor fluid uptake, HRP was used as a fluid-phase marker and cells were analyzed by electron microscopy or using an enzymatic assay to determine the amount of internalized HRP. For experiments in which HRP uptake was observed using electron microscopy, cultured mouse hepatocytes microinjected with either the anti-pan-dynamin antibody MC65 or heat-inactivated antibody were allowed to internalize HRP for 60 minutes, and were then processed for development of the HRP reaction product and electron microscopy as previously described (Henley et al., 1998). As shown in the micrograph in Fig. 4A and enlargement in Fig. 4A′, control cells microinjected with heat-inactivated antibody internalized substantial amounts of HRP into small, densely labeled endocytic compartments. By contrast, cells microinjected with native anti-pan-dynamin antibody (MC65) displayed very few HRP-positive endosomes (Fig. 4B,B′).

Depletion of Dyn2 protein through the use of *Dyn2* siRNA allowed us to inhibit Dyn2 function in a large population of cells simultaneously; thus, we could quantitate fluid uptake in cells treated in this manner using a biochemical method. Here, an enzymatic assay was used to determine HRP uptake in mock-treated versus *Dyn2*-siRNA-treated Clone 9 cells under low serum conditions or following stimulation with 10% FBS or EGF (30 ng/ml). In support of the morphological observations, HRP uptake was reduced by ~50% in *Dyn2*-siRNA-treated cells as compared to mock-treated cells under low serum conditions (0.2% FBS) (Fig. 4C). In addition,

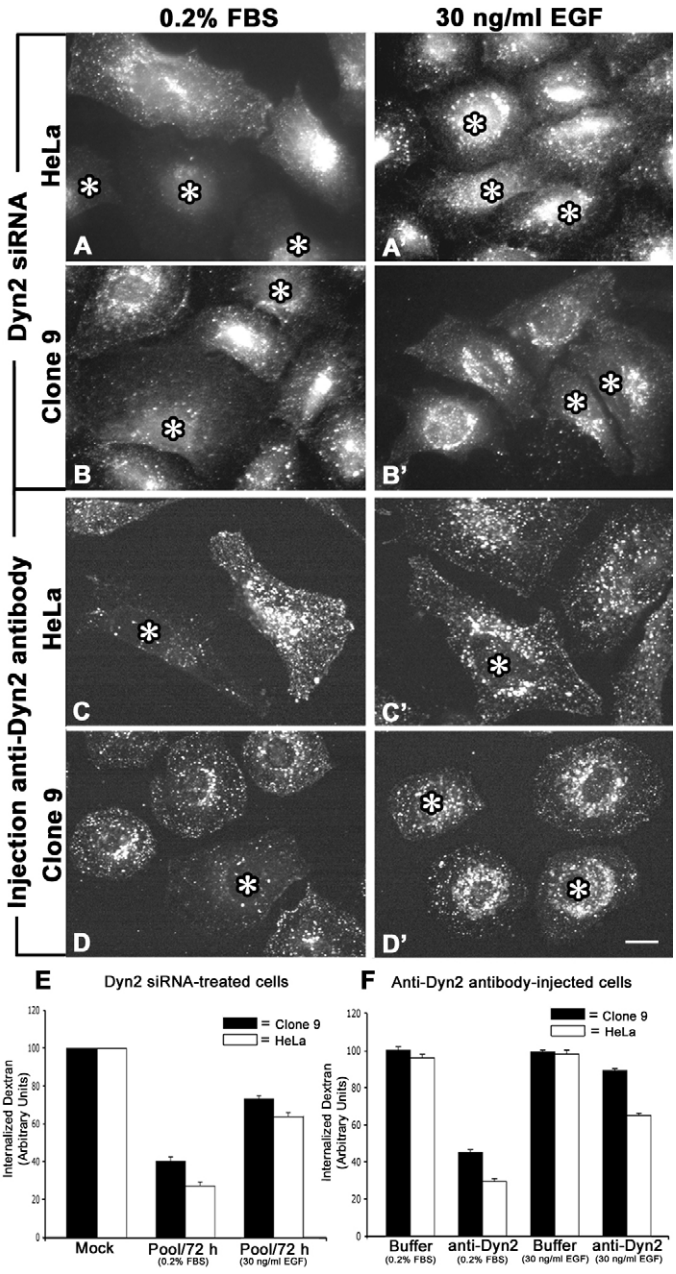

Fig. 3. Disruption of Dyn2 function in epithelial cells stimulated with EGF does not prevent macropinocytic internalization of fluid. (A-B′) Fluorescence micrographs of HeLa (A,A′) or Clone 9 (B,B′) cells treated with *Dyn2* siRNA for 72-96 hours prior to incubation with fluorescently conjugated dextran for 30 minutes in low serum medium (A,B) or low serum medium plus 30 ng/ml EGF (A′,B′). Cells with reduced Dyn2 levels (*) showed a marked reduction in fluid-phase endocytosis under unstimulated conditions, as compared with surrounding untransfected cells (A,B). Treatment of cells with EGF, however, induced a significant internalization of fluorescently conjugated dextran via the macropinocytic pathway, regardless of Dyn2 expression levels (A′,B′). (C-D′) Fluorescence micrographs of HeLa (C,C′) or Clone 9 (D,D′) cells microinjected with anti-Dyn2 antibodies as described in Fig. 1 and allowed to internalize fluorescently conjugated dextran under low serum conditions for 60 minutes in the absence (C,D) or presence (C′,D′) of EGF. As seen for *Dyn2*-siRNA-treated cells, dextran uptake was noticeably reduced in antibody-injected cells under low serum conditions (C,D), as compared with controls, whereas this effect was more modest in cells treated with EGF (C′,D′). (E,F) Quantitation of internalized fluorescently conjugated dextran in Clone 9 (black bars) and HeLa (white bars) cells treated with *Dyn2* siRNA (E) or microinjected with anti-Dyn2 antibodies (F) based on fluorescence intensity measurements. Values obtained from siRNA-treated cells were normalized to those of mock-treated cells under similar conditions, and values obtained from microinjected cells were normalized to those of surrounding uninjected cells. Results represent the average ± s.d. of ⩾50 cells measured in each of three independent experiments. Bar, 10 μm.

stimulation of cells with 10% FBS or EGF resulted in an increase in HRP internalization in mock-treated (~2-fold and ~1.7-fold, respectively) and in Dyn2 siRNA-treated (~2.5-fold and ~1.7-fold, respectively) cells, suggesting that Dyn2-independent processes contribute to growth-factor-stimulated fluid-phase uptake (Fig. 4C). Thus, both morphological and biochemical results indicate a role for Dyn2 in fluid-phase endocytosis under basal conditions.

Distinct Dyn2 spliced variants exhibit differential effects on fluid-phase endocytosis

The methods used above provided a general block of Dyn2 function; however, at least four spliced variants of Dyn2 are known to exist. These forms represent a substitution of a 38 amino acid cassette in the middle of the protein in which 13 residues are altered and an insertion/deletion of four amino acids immediately upstream of the pleckstrin homology (PH) domain (Cao et al., 1998) (Fig. 5, cartoon). Insertions/deletions upstream of the Dyn2 PH domain might lead to conformational changes, as has been predicted for the Dyn3 isoform (Gray et al., 2005), and thereby modulate the ability of specific Dyn2 spliced variants to interact with lipids and/or effector proteins. Thus, an interesting possibility is that specific spliced variants of Dyn2 preferentially participate in fluid-phase endocytosis.

We began analyzing the four Dyn2 spliced variants by observing the localizations of wild-type and GTPase mutant (K44A) versions of these proteins, some examples of which are shown in Fig. 5. When tagged with green fluorescent protein (GFP) and expressed in Clone 9 cells, the Dyn2 spliced variants showed both similarities and differences in their distributions. For example, although all spliced variants showed some association with clathrin-coated pits, there was a more impressive colocalization between clathrin and either Dyn2(aa) or Dyn2(ab) at the plasma membrane (Fig. 5A,B, insets) than between clathrin and Dyn2(ba) (Fig. 5C, inset). In addition, the GTPase mutant versions of the spliced variants also exhibited some differences in their localization patterns. Here, cells expressing untagged Dyn2(aa)K44A or Dyn2(ba)K44 formed large, punctate cytoplasmic structures and perinuclear aggregates (Fig. 5A′,C′), whereas cells expressing Dyn2(ab)K44A displayed long, linear membrane tubules that extended from the cell periphery towards the cell center and at times were associated with a clathrin bulb (Fig. 5B′, inset). Thus, even small insertions/deletions or changes in a few amino acids appear to play a role in the distribution of the different Dyn2 spliced variants.

The differences in cellular localization patterns suggested that the Dyn2 spliced variants could be, at least in part, selectively involved in distinct endocytic processes. Thus, we

tested whether expression of K44A GTPase mutants of the Dyn2 spliced variants affected transferrin and/or fluid-phase endocytosis in a spliced-variant-specific manner. Expression of GFP-tagged wild-type Dyn2(aa) in Clone 9 cells had no effect on transferrin internalization (Fig. 6A,A′), whereas expression of its mutant counterpart, Dyn2(aa)K44A (Fig. 6B), and expression of the Dyn2(ab)K44A mutant (Fig. 6C), reduced transferrin internalization by ~70% (Fig. 6B′,C′,D). A slightly less-potent inhibition was observed (~55%) in cells expressing either of the spliced-variant mutants Dyn2(ba)K44A or Dyn2(bb)K44A (Fig. 6D).

In contrast to the general inhibitory effects exhibited by Dyn2 GTPase mutants on clathrin-mediated endocytosis regardless of spliced variant, expression of Dyn2 spliced variants of the 'ba' or 'bb' form more selectively altered fluid-phase endocytosis. Interestingly, expression of wild-type Dyn2(ba) or Dyn2(bb) actually potentiated dextran internalization by ~15-20% under low serum conditions, as compared with surrounding untransfected cells and cells expressing wild-type Dyn2(aa) or Dyn2(ab) (Fig. 6H). Accordingly, dextran internalization was reduced by ~45% in cells expressing the Dyn2(ba)K44A mutant (Fig. 6F,F′,H) and by ~30% in cells expressing the Dyn2(bb)K44A mutant, as compared with untransfected cells (Fig. 6G,G′,H). By contrast, K44A mutant versions of Dyn2(aa) (Fig. 6E,E′) and Dyn2(ab) (images not shown) had no or only a modest effect on fluid-phase endocytosis (Fig. 6H). It is interesting that the forms most efficacious towards inhibiting transferrin uptake had no effect on fluid-phase endocytosis, whereas the reciprocal was observed for those forms that attenuated fluid-phase endocytosis. As observed when *Dyn2*-siRNA treatment was used to inhibit Dyn2 function, the presence of 10% FBS in the culture medium reduced the inhibitory effects of Dyn2(ba)K44A on fluid-phase endocytosis (~45% reduction in low serum versus ~15% reduction in 10% FBS; Fig. 6H, gray bar).

To further investigate whether specific Dyn2 spliced variants might be more efficacious in mediating fluid-phase endocytosis, we tested the ability of each of the four Dyn2 spliced variants to 'rescue' dextran uptake in *Dyn2*-siRNA-treated cells upon re-expression. Clone 9 cells were mock-treated, as a control, or treated with *Dyn2* siRNA for 48 hours to reduce Dyn2 protein levels. Subsequently, cells were transfected with a construct encoding for one of the four Dyn2 spliced variants and, following a 24-hour recovery, cells were assayed for dextran uptake (Fig. 7). Mock-treated cells exhibited a normal punctate Dyn2 staining pattern and internalized dextran to a perinuclear compartment, as expected (Fig. 7A,A′). In addition, endogenous Dyn2 levels were reduced in cells treated with *Dyn2* siRNA (Fig. 7B-C′, untransfected cells, and Fig. 7D), and cells depleted of Dyn2 internalized relatively little dextran (Fig. 7B-C′, untransfected cells, and Fig. 7E). By contrast, cells expressing high levels of exogenous Dyn2(ba) or Dyn2(bb) internalized large amounts of dextran, comparable to that of mock-treated cells (Fig. 7A-C′,E). Moreover, this 'rescue' effect was only apparent upon re-expression of these two specific Dyn2 spliced variants, Dyn2(ba) and Dyn2(bb) (Fig. 7E). Notably, expression of the K44A mutant versions of these spliced variants also resulted in the greatest inhibitory effects on dextran uptake (Fig. 6H). Together, these observations support the idea that Dyn2 mediates basal fluid-phase endocytosis and, additionally, that specific Dyn2 spliced variants differentially affect specific forms of endocytosis.

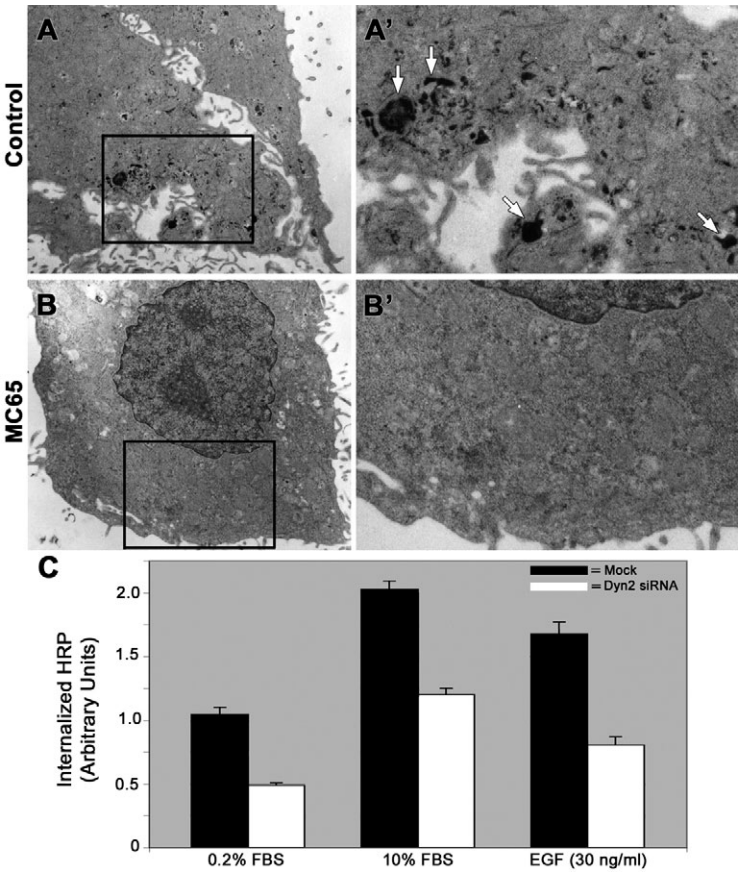

Fig. 4. Inhibition or depletion of Dyn2 reduces internalization of the fluid-phase marker HRP. (A-B′) Electron micrographs of HRP uptake in mouse hepatocytes (BNL CL.2) microinjected with control heat-inactivated antibody (A; A′, enlargement of boxed area) or the anti-pan-dynamin antibody MC65 (B; B′, enlargement of boxed area). Numerous HRP-positive endosomes were detected in control cells following a 60-minute incubation with HRP (A′, arrows); however, cells microinjected with native antibody (MC65) displayed very few HRP-positive endocytic structures (B,B′), indicating inhibition of fluid-phase uptake. (C) Quantitation of HRP uptake in mock-treated (black bars) or *Dyn2*-siRNA-treated (white bars) Clone 9 cells under the indicated serum conditions based on HRP enzyme activity using *o*-phenylenediamine as a substrate. The ratio of HRP enzyme activity (absorbance at 490 nm) to protein concentration (absorbance at 600 nm) was determined for each sample and is presented as arbitrary units. The amount of internalized HRP was reduced in cells treated with *Dyn2* siRNA under all serum conditions when compared with mock-treated cells under similar conditions, although stimulation with 10% FBS or with EGF appeared to induce Dyn2-independent mechanisms of fluid uptake. Results represent the average ± s.d. for three independent experiments.

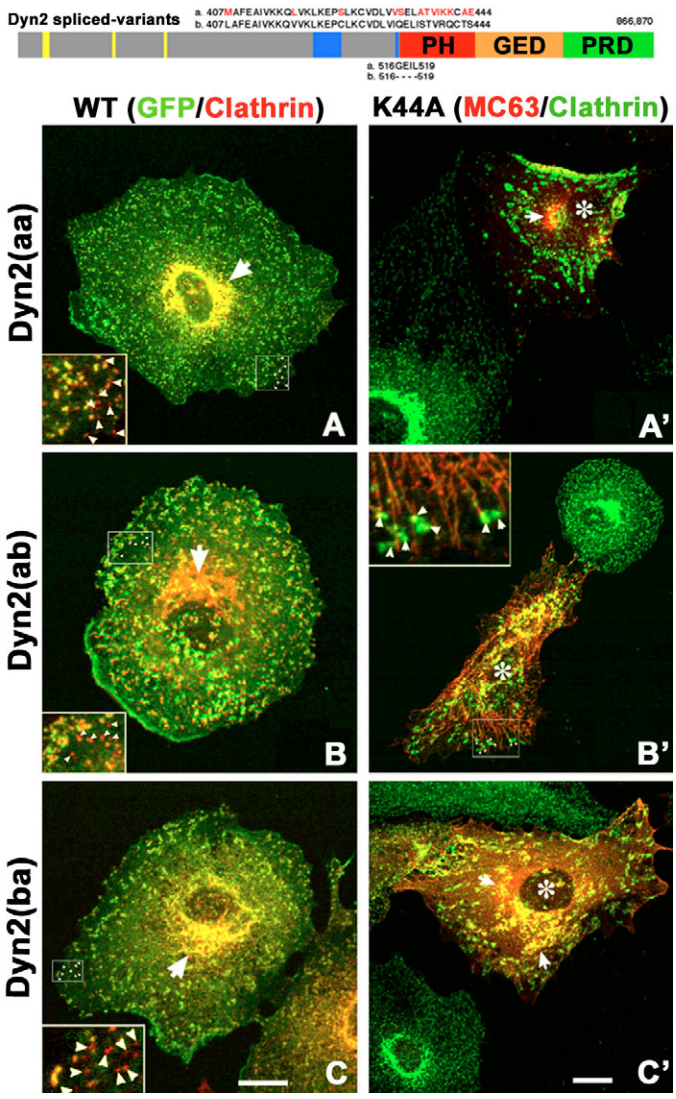

Fig. 5. Differential distribution of wild-type and GTPase mutant Dyn2 spliced variants. (Top) Cartoon of the Dyn2 protein showing the tripartite GTP-binding motif (yellow) and the substitution/deletion sequences of the distinct spliced variants. Red lettering indicates amino acids that differ between the 'a' and 'b' Dyn2 spliced variants in the first splicing cassette. Other domains of the Dyn2 protein indicated are the pleckstrin homology domain (PH), guanine nucleotide exchange domain (GED) and proline-rich domain (PRD). (A,B,C) Fluorescence micrographs of Clone 9 cells expressing GFP-tagged wild-type (WT) versions of the indicated Dyn2 spliced variants (green) that were fixed and immunostained for clathrin (red). The different Dyn2 spliced variants show varying degrees of association with clathrin, both at the plasma membrane (insets) and at the perinuclear Golgi region (arrows). (A′,B′,C′) Fluorescence micrographs of Clone 9 cells expressing untagged GTPase mutant (K44A) versions of the different Dyn2 spliced variants that were fixed and immunostained with anti-pan-dynamin (MC63, red) and anti-clathrin (green) antibodies. Two distinct phenotypes were generally observed, including either a perinuclear concentration of mutant Dyn2 protein (A′,C′, arrows) or long, linear, tubular structures terminating in a prominent clathrin-coated tip (B′; arrowheads in inset). (*) Indicates a transfected cell. Bars, 10 μm.

Discussion

In this study we examined the role of Dyn2 and its spliced variants in different endocytic processes in epithelial cells. The strengths of this study lie in the variety of Dyn2 probes and epithelial cell lines used. Our experimental approach first provided a general, but specific, block for all Dyn2 spliced variants in the cells tested through microinjection of purified polyclonal antibodies. These reagents were previously shown to inhibit the Dyn2-dependent internalization of transferrin by clathrin-coated pits or cholera toxin B by caveolae (Henley et al., 1998), and we now show that they also have a marked inhibitory effect on dextran uptake (Figs 1 and 3, and supplementary material Fig. S1). As a second general inhibitory method, siRNA was used to reduce Dyn2 protein levels in cells, and this also resulted in an attenuation of not only transferrin uptake but also of the internalization of the fluid-phase markers dextran and HRP (Figs 2-4, and supplementary material Fig. S2). Importantly, the inhibitory effects of depleting Dyn2 protein on fluid uptake could be quantitated both morphologically, based on fluorescence intensity measurements, and biochemically, by assaying HRP enzyme activity. Indeed, results from both of these methods support that Dyn2 plays a role in fluid-phase endocytosis, especially under low serum conditions, whereas stimulation with serum or growth factors appeared to upregulate Dyn2-independent endocytic processes (Figs 2-4). In addition, the effects of disrupting Dyn2 function on fluid-phase endocytosis did not appear to be an indirect result of the role of Dyn2 in clathrin- or caveolae-mediated endocytosis, because siRNA-mediated reduction of clathrin and caveolin-1 protein levels did not affect fluid-phase endocytosis (supplementary material Fig. S3). However, disruption of one endocytic pathway might stimulate a compensatory pathway (Damke et al., 1995), making these results more difficult to interpret, and all forms of endocytosis most probably involve at least some internalization of fluid under normal conditions. Thus, clathrin- and caveolin-dependent endocytosis might also be a component of Dyn2-mediated fluid uptake.

Following the use of these broad Dyn2 inhibitory reagents, we next tested whether a distinct Dyn2 spliced variant might preferentially mediate fluid-phase endocytosis. Expression and analysis of wild-type and K44A GTPase mutant Dyn2 spliced variants showed that these proteins not only exhibit distinct cellular localizations (Fig. 5), but do indeed also differentially affect dextran uptake (Figs 6 and 7). Together, our findings suggest that: (1) Dyn2 is involved in the internalization of fluid-phase markers (dextran and HRP) under low serum conditions in multiple epithelial cell types; (2) stimulation with high levels of serum or growth factors upregulates Dyn2-independent mechanisms of fluid-phase endocytosis; and (3) distinct spliced variants of Dyn2 exhibit differential cytoplasmic localizations and effects on fluid uptake.

The results presented here are in agreement with the initial ~50% reduction in HRP uptake observed by Damke et al. following inhibition of Dyn1 function using a temperature-sensitive mutant (Damke et al., 1995) and the ~60% reduction observed by Macia et al. in cells treated with the small molecule inhibitor dynasore (Macia et al., 2006). However, Damke et al. also observed a subsequent upregulation of

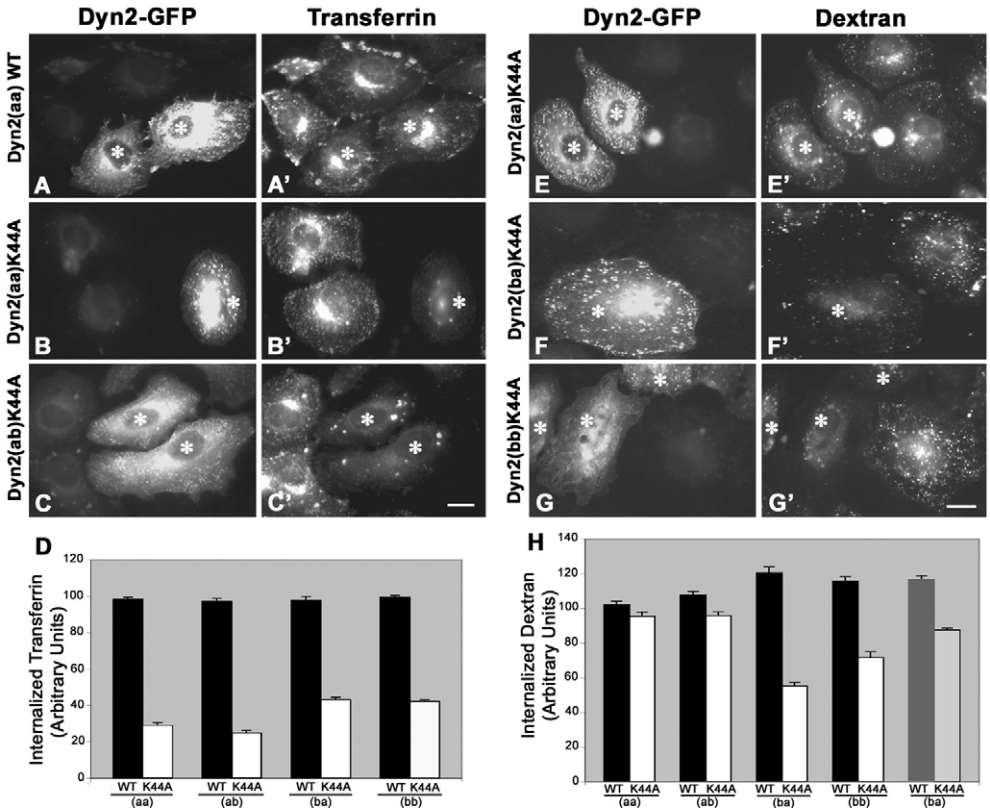

Fig. 6. Inhibition of fluid-phase endocytosis in Clone 9 cells by specific Dyn2 spliced variant mutants. (A-C′,E-G′) Fluorescence micrographs of Clone 9 cells expressing either GFP-tagged wild-type (A, WT) or K44A GTPase mutant (B,C,E,F,G) forms of the different Dyn2 spliced variants that had been incubated with either fluorescently conjugated transferrin (A′,B′,C′) or dextran (E′,F′,G′). Internalization of dextran was assayed under low serum conditions. Expression of GFP-tagged wild-type Dyn2(aa) (A) did not alter transferrin internalization (A′), whereas expression of the K44A mutant of this Dyn2 spliced variant (B) or the Dyn2(ab) spliced variant (C) did inhibit transferrin uptake (B′,C′). By contrast, expression of Dyn2(aa)K44A (E) did not inhibit dextran uptake, even under low serum conditions (E′). However, expression of K44A mutant versions of two Dyn2 spliced variants, Dyn2(ba) (F) and Dyn2(bb) (G), did attenuate dextran internalization under low serum conditions (F′,G′). (*) Indicates a transfected cell. (D,H) Quantitation of transferrin (D) and dextran (H) internalization in cells expressing wild-type (black bars) or K44A mutant (white bars) versions of the different Dyn2 spliced variants based on fluorescence intensity measurements. Although mutant forms of all of the Dyn2 spliced variants reduced the internalization of transferrin (D), the effects on dextran uptake (fluid-phase endocytosis) appeared to depend on the Dyn2 spliced variant being expressed (H). As occurred when other methods were used to inhibit Dyn2 function, the inhibitory effects of Dyn2(ba)K44A expression on the internalization of dextran were reduced when cells were assayed in the presence of 10% FBS (H, gray bars). Values obtained from cells expressing Dyn2 constructs were normalized to those of surrounding untransfected cells. Results represent the average ± s.d. of ⩾50 cells measured in each of three independent experiments. Bars, 10 μm.

dynamin-independent fluid uptake in cells incubated at the restrictive temperature for prolonged times (30-120 minutes), such that the levels of internalized HRP were equal to or more than that of control cells (Damke et al., 1995), a phenotype not noted in our studies. Possibly the distinct methods of inhibiting Dyn2 function and/or time-frames of analysis can account for some of the differences in results. For example, analysis of HRP uptake in cells expressing either a Dyn1K44A or Dyn2K44A mutant, as opposed to the Dyn1 temperature-sensitive mutant, did not reveal a stimulation of dynamin-independent fluid uptake (Altschuler et al., 1998; Damke et al., 1994). Another apparent contradiction with our observations here lies with results from a recent study by Schlunck et al., who found that Dyn2 does not participate in basal fluid-phase endocytosis but does mediate macropinocytosis in platelet-derived growth factor (PDGF)-stimulated fibroblasts (Schlunck et al., 2004). This observation could be attributed to the fact that PDGF stimulation of fibroblasts induces the formation of large dorsal ruffles that represent a distinct Dyn2-dependent endocytic pathway used to internalize fluid and growth-factor-stimulated receptors (Krueger et al., 2003; Orth and McNiven, 2006). As indicated in the Introduction, additional examples of Dyn2-independent mechanisms of fluid-phase endocytosis exist, such as the Cdc42-dependent pathway used to internalize GPI-linked proteins and CtBP3/BARS-mediated pathways (Bonazzi et al., 2005; Kirkham et al., 2005; Sabharanjak et al., 2002). Indeed, multiple pathways of fluid internalization certainly exist, some of which are Dyn2-dependent, whereas others are not. These different pathways are used to various degrees depending on the cellular conditions. Regardless, our consistent results here using multiple methods of inhibition (*Dyn2* siRNA, anti-dynamin antibody microinjection and expression of Dyn2 GTPase mutants), a variety of epithelial cell types, and both morphological and biochemical assays for detecting fluid uptake strongly support that Dyn2 is involved in coat-independent micropinocytosis of fluid.

Dynamin variants: splicing matters

A particularly interesting observation made here is the differential contributions of the four Dyn2 spliced variants to distinct endocytic pathways. Whereas GTPase mutants of the Dyn2(ba) and Dyn2(bb) spliced variants had a greater effect on dextran uptake, mutation of the Dyn2(aa) and Dyn2(ab) spliced variants had a greater effect on transferrin uptake (Fig. 6). In further support of different roles for specific Dyn2 spliced variants in distinct endocytic pathways, it has been shown that the proline-rich domain (PRD) of the Dyn2(aa)

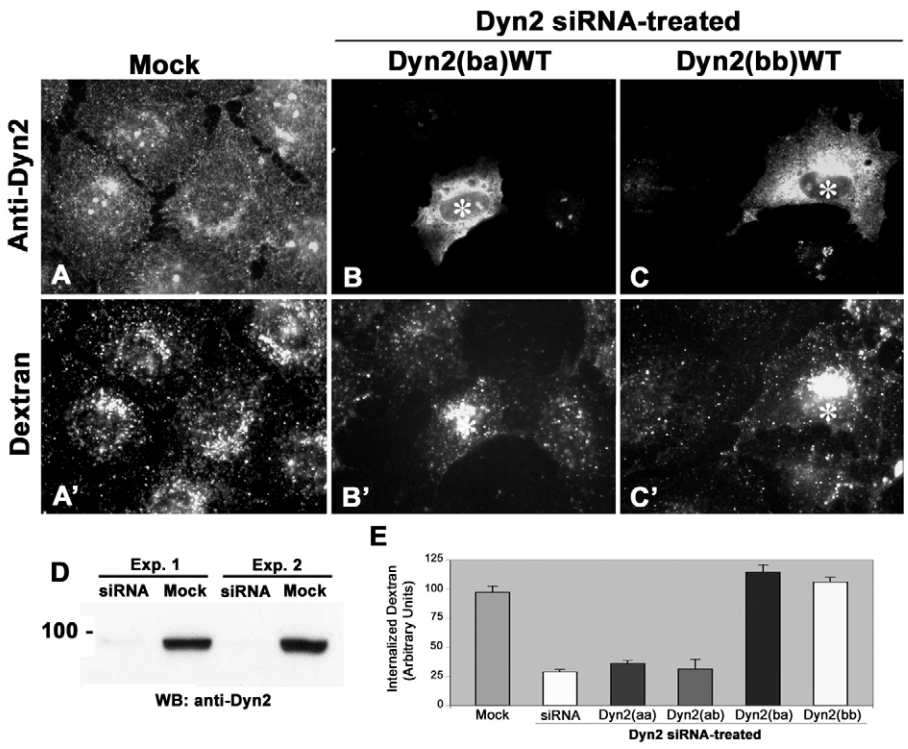

Fig. 7. Expression of either of two specific Dyn2 spliced variants, Dyn2(ba) or Dyn2(bb), rescues fluid-phase endocytosis in *Dyn2*-siRNA-treated cells. (A,A′) Fluorescence micrographs of Clone 9 cells treated with transfection reagent alone (Mock) that were allowed to internalize fluorescently conjugated dextran for 60 minutes under low serum conditions and were subsequently immunostained for Dyn2. Mock-treated cells show a punctate plasma membrane and Golgi localization of Dyn2 (A), and a perinuclear accumulation of dextran-positive cytoplasmic vesicles (A′). (B-C′) Clone 9 cells were treated with *Dyn2* siRNA for 48 hours and then transfected with constructs encoding untagged versions of the different Dyn2 spliced variants. Twenty-four hours later, cells were assayed for dextran internalization and immunostained for Dyn2. Fluorescence micrographs of *Dyn2*-siRNA-treated cells re-expressing either Dyn2(ba) (B, asterisk) or Dyn2(bb) (C, asterisk) show that dextran uptake has been 'rescued' in these cells (B′,C′), whereas surrounding cells still depleted of Dyn2 internalize relatively little dextran. (D) Western blot analysis of Dyn2 protein levels in siRNA- and mock-treated cells performed in parallel with the rescue experiments. (E) Quantitation of dextran uptake in cells treated with reagent alone (Mock), *Dyn2* siRNA, or *Dyn2* siRNA followed by re-expression of the indicated Dyn2 spliced variants based on fluorescence intensity units. All images were acquired and adjusted equally, allowing for a comparison among all conditions. Results represent the average ± s.d. of ⩾50 cells measured in each of two independent experiments.

spliced variant, but not of the Dyn2(bb) spliced variant, strongly binds the C-terminal cytoplasmic region of caveolin-1 in vitro. Moreover, expression of the Dyn2(aa)K44A mutant inhibited the internalization of cholera toxin B, whereas expression of Dyn2(bb)K44A did not (Yao et al., 2005). Because the PRDs of all of the Dyn2 spliced variants are identical in sequence, this observation suggests that an insertion within the Dyn2(aa) spliced variant might change the conformation of Dyn2 to extend the PRD outward in such a way as to make it more accessible for interactions with caveolin-1. Such a model has been postulated for the Dyn3 spliced variants, which are expressed largely in brain and are thought to participate in dendritic spine morphogenesis via an interaction with cortactin (Gray et al., 2005). Interestingly, one spliced variant of Dyn3, Dyn3(aaa), when expressed in neurons, has very little effect on neuronal morphology; however, another spliced variant, Dyn3(baa), which only has a modest ten amino acid insertion immediately upstream of the PH domain, induces dramatic changes in spine morphology. Computer modeling of the Dyn3(baa) spliced variant predicts that the insertion could result in a profound protrusion of the Dyn3 PH domain, making it more available for interactions with lipids or effector proteins. As shown in the cartoon in Fig. 5, the Dyn2 spliced variants studied here also differ by a substitution (amino acids 407-444) and/or insertion (amino acids 516-519) immediately upstream of the PH domain (amino acids 522-623) – differences that are likely to be essential in targeting the different spliced variants to distinct cytoplasmic locations. Furthermore, inducing the presence or absence of a specific substitution and/or insertion through splicing might also be involved in the different phenotypes observed upon expression of GTPase mutants of the Dyn2 spliced variants (Figs 5 and 6). Indeed, expression of mutant Dyn2 proteins containing spontaneous mutations near these Dyn2 splicing regions in specific human ethnic populations results in membrane-cytoskeletal alterations in neurons and, subsequently, phenotypic neuropathies (Zuchner et al., 2005).

The use of various dynamin isoforms and spliced variants by others might provide some insight into the inconsistencies reported regarding the role of dynamin in fluid-phase endocytosis. As mentioned earlier, electron-microscopy analysis of HRP internalization in temperature-shifted *shibire*^{ts} flies demonstrated a considerable decrease in this process at the restrictive temperature, but not at the permissive temperature (Kosaka and Ikeda, 1983). This study was particularly attractive because all dynamin gene products, regardless of splicing, would be rendered inactive at the restrictive temperature, providing a general block in dynamin function. However, analysis of fluid-phase endocytosis in cultured cells from *shibire*^{ts} larvae did not indicate a decrease in this form of endocytosis at the restrictive temperature, suggesting that this pathway might be dynamin-independent (Guha et al., 2003). It appears that several factors are essential in measuring the effects of dynamin on fluid-phase endocytosis. These include inhibiting all dynamin forms present in the cells being analyzed; paying careful attention to the specific spliced variant being expressed when a dominant-negative approach is used to inhibit Dyn2 function; and serum-

starving cells for 16-24 hours prior to dextran addition and performing endocytic assays in low serum medium to minimize Dyn2-independent macropinocytic processes. The demonstration here that Dyn2 is involved in fluid-phase endocytosis opens the door to many additional questions regarding interactions between Dyn2 and components involved in distinct types of vesicle formation. In addition, it will be interesting to analyze potential additional functions specific to the different Dyn2 spliced variants and how they are regulated.

Materials and Methods

Reagents and antibodies

MiniPrep Express Matrix and Luria-Bertani medium were from BIO 101 (Vista, CA). Restriction enzymes and 1 kb DNA Ladder were from New England Biolabs (Beverly, MA). The anti-clathrin monoclonal antibody X22 was collected from the supernatant of the X22 hybridoma cell line (ATCC, Rockville, MD). The anti-kinesin antibody MC44 has been previously characterized (Cao et al., 2003; Henley and McNiven, 1996; Marks et al., 1994). The anti-pan-dynamin MC63 (Henley and McNiven, 1996) and MC65 (Henley et al., 1998) antibodies were made against peptides covering conserved regions of Dyn1 and Dyn2. The anti-Dyn2 antibody was made against a peptide covering a C-terminal region present only in Dyn2 (Henley et al., 1998). The anti-caveolin-1 polyclonal antibody was made against an N-terminal peptide present in rat alpha-caveolin-1 (amino acids 5-33): KYVDSEGHLYTVPIREQGNIYKPNNKAMA. All antibodies were affinity purified before use, as previously described (Henley and McNiven, 1996). Goat anti-rabbit and goat anti-mouse secondary antibodies conjugated to either Alexa-Fluor-488 or -594; transferrin Alexa-Fluor-488 and -594; Rhodamine- and FITC-dextran (3000 MW); and cholera toxin B Alexa-Fluor-488 used for immunofluorescent staining were from Molecular Probes (Eugene, OR). EGF, HRP (type VI) and *o*-phenylenediamine were from Sigma (St Louis, MO).

Cell culture and transfection

Clone 9 cells, an epithelial cell line isolated from normal rat liver (ATCC CRL-1439, Rockville, MD), were maintained in Ham's F12-K medium; BNL CL.2, normal mouse liver cells (ATCC TIB 73), were maintained in DMEM; and HeLa cells (ATCC CCL-2) and MDCK (NBL-2) cells (ATCC CCL-34) were maintained in DMEM containing 1.0 mM sodium pyruvate, 0.1 mM nonessential amino acids and 1.5 g/L sodium bicarbonate. All media were supplemented with 10% FBS (Invitrogen, Carlsbad, CA), 100 U/ml penicillin and 100 μg/ml streptomycin. Cells were cultured at 37°C in 5% CO_2/95% air in T-75 flasks (Fisher Scientific, Pittsburgh, PA). Confluent cells were trypsinized (1× Trypsin-EDTA, 0.25% Trypsin, 1 mM EDTA, Invitrogen) and cultured on 22-mm coverslips prior to transfection with plasmid DNA and/or siRNA oligonucleotides. Dyn2 constructs (1-2 μg) were transfected using the Lipofectamine Plus Reagent kit (Invitrogen), and siRNA oligonucleotides were transfected using the Oligofectamine Reagent kit (Invitrogen), both according to the manufacturer's instructions. Subsequently, cells were stained using standard immunofluorescence procedures or assayed for uptake of various endocytic markers. For rescue experiments, Clone 9 cells were treated with *Dyn2* siRNA oligonucleotides for 48 hours and then transfected with constructs encoding wild-type versions of the different Dyn2 spliced variants using the Lipofectamine 2000 Reagent kit (Invitrogen). At 24 hours post-transfection of Dyn2 constructs, cells were assayed for dextran uptake.

Plasmid construction

GFP-tagged and untagged Dyn2 wild-type and mutant constructs were generated as previously described (Cao et al., 1998). All DNA constructs were verified by restriction-enzyme digestion and sequence analysis [The Mayo Molecular Biology Core (ABI PRISM 377 DNA sequencer, Perkin Elmer-Cetus), Rochester, MN]. Sequences were analyzed using DNA* analysis software (DNA star, Madison, WI). Dyn2 plasmid DNAs were purified either by equilibrium centrifugation in a CsCl-ethidium bromide gradient (Cao et al., 1998) or Qiagen Plasmid Maxi kit (Qiagen, Valencia, CA).

Small interfering RNA oligonucleotides

siRNA oligonucleotides targeting four different regions of *Dyn2* were purchased from Dharmacon Research (Lafayette, CO) and pooled before being transfected to mediate reduction of Dyn2 protein levels. The four target sequences, selected by Dharmacon Research, were as follows: #1 5′-GUACAAGGAUGAAGAGGAA-3′; #2 5′-GACAUGAUCCUGCAGUUUA-3′; #3 5′-GAGAGCAGCCUCAUUCUUG-3′; and #4 5′-GAGCUCAUCCCGCUGGUUA-3′. The caveolin-1 siRNA target sequence used was 5′-AACCAGAAGGGACACACAGUU-3′. The clathrin siRNA target sequence used was 5′-GCAAUGAGCUGUUUGAAGAUU-3′. The oligonucleotides were received in an annealed and purified form ready to be transfected upon resuspension in OPTI-MEM I (GIBCO BRL, Grand Island, NY).

Microinjection of antibodies

Clone 9, MDCK, BNL CL.2 and HeLa cells were microinjected with either buffer alone (10 mM KH_2PO_4, pH 7.2, and 75 mM KCL) or buffer containing one of the following antibodies at the indicated concentration: anti-pan-dynamin (MC65; 7.2 mg/ml), anti-Dyn2 (8.6 mg/ml) or anti-kinesin (MC44; 7.8 mg/ml). Fixable Rhodamine- or FITC-conjugated dextran was included in the injectate in order to identify the injected cells. The cells were allowed to recover in 5% CO2/95% air at 37°C for 4-6 hours prior to assaying endocytic function.

Assays for Internalization of cholera toxin B, dextran and transferrin

Endocytosis of fluorescently conjugated transferrin or cholera toxin B was assayed as previously described (Henley et al., 1998; Yao et al., 2005). Fluid-phase endocytosis was assayed using Rhodamine-conjugated dextran (3000 MW). Cells were either microinjected, treated with siRNA or transfected with Dyn2 constructs before assays were performed. Cells were maintained at 5% CO_2/95% air at 37°C in medium supplemented with 10% FBS (high serum medium) or 0.2% FBS (low serum medium) for 16-24 hours then incubated with 150 mM Rhodamine-conjugated dextran for 60 minutes. For microinjection experiments when low serum medium was used, cells were switched to low serum medium for 4-6 hours following microinjection before being assayed. EGF-stimulated cells were cultured in low serum medium for 16 hours then exposed to 30 ng/ml EGF along with 150 mM Rhodamine-conjugated dextran for 30 minutes. After incubation, cells were rinsed with HBSS three times followed by rinsing with 0.5 N $NaCl_2$ in HBSS for 1 minute to reduce background.

Immunofluorescence and microscopy

Cells were processed for immunofluorescence and viewed using either an epifluorescence or confocal microscope as previously described (Cao et al., 1998). All images were adjusted and assembled into figures using Adobe Photoshop (Adobe systems, Mountainview, CA).

Morphological quantitation of endocytic uptake

All images of microinjected cells, siRNA-treated cells or wild-type- or mutant-Dyn2-expressing cells were acquired using a cooled CCD camera (Photometrics SenSys, Tuscon, AZ) at full resolution using the same acquisition settings (exposure time=500 mseconds, 16 bit grayscale). To quantitate fluorescence intensity, the area of each cell was traced, and the mean fluorescence intensity per unit area was determined using IP Lab software (Scanalytics, Fairfax, VA). The results presented represent the average fluorescence intensity units ± s.d. measured for ⩾50 cells for each of two to four independent experiments.

HRP uptake assay

For a biochemical analysis of fluid uptake, Clone 9 cells were grown on 10-cm dishes and mock-treated with transfection reagent alone or treated with *Dyn2* siRNA for 72 hours. During this time, 16 hours prior to assaying for fluid uptake, cells were incubated in low serum medium (0.2% FBS). Subsequently, cells were incubated with HRP (1 mg/ml) under low serum conditions or in medium containing 10% FBS or EGF (30 ng/ml) for 1 hour at 37°C. Uptake of HRP was stopped by quickly aspirating the medium, followed by two washes with HBSS and treatment of cells with 0.05% Trypsin-EDTA to detach cells and remove residual HRP non-specifically bound to the plasma membrane. After resuspension in HBSS, cells were collected in a 15-ml Falcon tube and spun at 1100 ***g*** for 3 minutes. Cells were then washed once more with HBSS and twice with ice-cold PBS, spinning down at 1100 ***g*** between washes. After transferring cells to a 1.5-ml Eppendorf tube followed by a brief pelleting, cells were incubated with 1 ml of buffer containing 1 mM $MgCl_2$, 1 mM $CaCl_2$ and 0.2% BSA (pH 7.4) for 5 minutes on ice and then washed twice more with ice-cold PBS, spinning down at 800 ***g*** for 3 minutes between washes. After the final wash, the cell pellets were resuspended in 500 μl of ice-cold PBS containing 0.1% Triton X-100 and sonicated on ice four times using 1-minute pulses. The samples were then spun down at 16,000 ***g*** for 5 minutes in the cold to remove cell debris, and the supernatants were transferred to a fresh tube prior to assaying for HRP enzyme activity using *o*-phenylenediamine as a chromogenic substrate. Assays were conducted in a 96-well microplate by adding 2 μl of lysate to 100 μl of 0.5 N NaHCOOH (pH 5.0) containing 0.75 mg/ml *o*-phenylenediamine and 0.006% H_2O_2 (made fresh). The reaction was allowed to proceed for 5 minutes at room temperature and was then stopped by adding 100 μl of 0.1 N H_2SO_4. The amount of reaction product generated was determined by measuring the sample absorbance at 490 nm, and this was normalized to the protein concentration (absorbance at 600 nm), which was determined using the MicroBCA assay (Pierce Chemical, Rockford, IL). Results are presented as arbitrary units based on the 490:600 nm absorbance ratio and represent the average ± s.d. for three independent experiments.

Electron microscopy

Mouse hepatocytes (BNL CL.2 cells) were plated onto carbon-coated, glow discharged coverslips for 24 hours in DMEM with 10% FBS and then injected with anti-pan-dynamin antibody (MC65) or heat-inactivated antibody, as a control, as

previously described (Henley et al., 1998). After a 4-6 hour recovery, cells were incubated with 5.3 mg/ml HRP (Sigma) in DMEM with 10% FBS +5 mM HEPES, pH 7.2, for 60 minutes at 37°C. After washing twice with cold HBSS +5 mM HEPES, pH 7.2, cells were briefly placed into medium again for 5 minutes, and subsequently fixed and processed for development of the HRP reaction product as previously described (Henley et al., 1998).

Thanks to E. W. Krueger for help with experiments where cells were imaged using electron microscopy and to H. M. Thompson for help in preparing the manuscript. This work was supported by a grant from the National Institutes of Health to M.A.M. (DK 44650).

References

Altschuler, Y., Barbas, S. M., Terlecky, L. J., Tang, K., Hardy, S., Mostov, K. E. and Schmid, S. L. (1998). Redundant and distinct functions for dynamin-1 and dynamin-2 isoforms. *J. Cell Biol.* **143**, 1871-1881.

Bonazzi, M., Spano, S., Turacchio, G., Cericola, C., Valente, C., Colanzi, A., Kweon, H. S., Hsu, V. W., Polishchuck, E. V., Polishchuck, R. S. et al. (2005). CtBP3/BARS drives membrane fission in dynamin-independent transport pathways. *Nat. Cell Biol.* **7**, 570-580.

Cao, H., Garcia, F. and McNiven, M. A. (1998). Differential distribution of dynamin isoforms in mammalian cells. *Mol. Biol. Cell* **9**, 2595-2609.

Cao, H., Orth, J. D., Chen, J., Weller, S. G., Heuser, J. E. and McNiven, M. A. (2003). Cortactin is a component of clathrin-coated pits and participates in receptor-mediated endocytosis. *Mol. Cell. Biol.* **23**, 2162-2170.

Conner, S. D. and Schmid, S. L. (2003). Regulated portals of entry into the cell. *Nature* **422**, 37-44.

Damke, H., Baba, T., Warnock, D. E. and Schmid, S. L. (1994). Induction of mutant dynamin specifically blocks endocytic coated vesicle formation. *J. Cell Biol.* **127**, 915-934.

Damke, H., Baba, T., van der Bliek, A. M. and Schmid, S. L. (1995). Clathrin-independent pinocytosis is induced in cells overexpressing a temperature-sensitive mutant of dynamin. *J. Cell Biol.* **131**, 69-80.

Gray, N. W., Kruchten, A. E., Chen, J. and McNiven, M. A. (2005). A dynamin-3 spliced variant modulates the actin/cortactin-dependent morphogenesis of dendritic spines. *J. Cell Sci.* **118**, 1279-1290.

Guha, A., Sriram, V., Krishnan, K. S. and Mayor, S. (2003). Shibire mutations reveal distinct dynamin-independent and -dependent endocytic pathways in primary cultures of Drosophila hemocytes. *J. Cell Sci.* **116**, 3373-3386.

Henley, J. R. and McNiven, M. A. (1996). Association of a dynamin-like protein with the Golgi apparatus in mammalian cells. *J. Cell Biol.* **133**, 761-775.

Henley, J. R., Krueger, E. W., Oswald, B. J. and McNiven, M. A. (1998). Dynamin-mediated internalization of caveolae. *J. Cell Biol.* **141**, 85-99.

Herskovits, J. S., Burgess, C. C., Obar, R. A. and Vallee, R. B. (1993). Effects of mutant rat dynamin on endocytosis. *J. Cell Biol.* **122**, 565-578.

Hinshaw, J. E. (2000). Dynamin and its role in membrane fission. *Annu. Rev. Cell Dev. Biol.* **16**, 483-519.

Johannes, L. and Lamaze, C. (2002). Clathrin-dependent or not: is it still the question? *Traffic* **3**, 443-451.

Kirkham, M. and Parton, R. G. (2005). Clathrin-independent endocytosis: new insights into caveolae and non-caveolar lipid raft carriers. *Biochim. Biophys. Acta* **1746**, 349-363.

Kirkham, M., Fujita, A., Chadda, R., Nixon, S. J., Kurzchalia, T. V., Sharma, D. K., Pagano, R. E., Hancock, J. F., Mayor, S. and Parton, R. G. (2005). Ultrastructural identification of uncoated caveolin-independent early endocytic vehicles. *J. Cell Biol.* **168**, 465-476.

Kosaka, T. and Ikeda, K. (1983). Reversible blockage of membrane retrieval and endocytosis in the garland cell of the temperature-sensitive mutant of Drosophila melanogaster, shibirets1. *J. Cell Biol.* **97**, 499-507.

Kruchten, A. E. and McNiven, M. A. (2006). Dynamin as a mover and pincher during cell migration and invasion. *J. Cell Sci.* **119**, 1683-1690.

Krueger, E. W., Orth, J. D., Cao, H. and McNiven, M. A. (2003). A dynamin-cortactin-Arp2/3 complex mediates actin reorganization in growth factor-stimulated cells. *Mol. Biol. Cell* **14**, 1085-1096.

Macia, E., Ehrlich, M., Massol, R., Boucrot, E., Brunner, C. and Kirchhausen, T. (2006). Dynasore, a cell-permeable inhibitor of dynamin. *Dev. Cell* **10**, 839-850.

Marks, D. L., Larkin, J. M. and McNiven, M. A. (1994). Association of kinesin with the Golgi apparatus in rat hepatocytes. *J. Cell Sci.* **107**, 2417-2426.

Mayor, S. and Pagano, R. E. (2007). Pathways of clathrin-independent endocytosis. *Nat. Rev. Mol. Cell Biol.* **8**, 603-612.

McNiven, M. A., Cao, H., Pitts, K. R. and Yoon, Y. (2000). The dynamin family of mechanoenzymes: pinching in new places. *Trends Biochem. Sci.* **25**, 115-120.

Nichols, B. J. and Lippincott-Schwartz, J. (2001). Endocytosis without clathrin coats. *Trends Cell Biol.* **11**, 406-412.

Orth, J. D. and McNiven, M. A. (2003). Dynamin at the actin-membrane interface. *Curr. Opin. Cell Biol.* **15**, 31-39.

Orth, J. D. and McNiven, M. A. (2006). Get off my back! Rapid receptor internalization through circular dorsal ruffles. *Cancer Res.* **66**, 11094-11096.

Sabharanjak, S., Sharma, P., Parton, R. G. and Mayor, S. (2002). GPI-anchored proteins are delivered to recycling endosomes via a distinct cdc42-regulated, clathrin-independent pinocytic pathway. *Dev. Cell* **2**, 411-423.

Schafer, D. A. (2004). Regulating actin dynamics at membranes: a focus on dynamin. *Traffic* **5**, 463-469.

Schlunck, G., Damke, H., Kiosses, W. B., Rusk, N., Symons, M. H., Waterman-Storer, C. M., Schmid, S. L. and Schwartz, M. A. (2004). Modulation of Rac localization and function by dynamin. *Mol. Biol. Cell* **15**, 256-267.

Slepnev, V. I. and De Camilli, P. (2000). Accessory factors in clathrin-dependent synaptic vesicle endocytosis. *Nat. Rev. Neurosci.* **1**, 161-172.

Sontag, J. M., Fykse, E. M., Ushkaryov, Y., Liu, J. P., Robinson, P. J. and Sudhof, T. C. (1994). Differential expression and regulation of multiple dynamins. *J. Biol. Chem.* **269**, 4547-4554.

Staples, R. R. and Ramaswami, M. (1999). Functional analysis of dynamin isoforms in Drosophila melanogaster. *J. Neurogenet.* **13**, 119-143.

Swanson, J. A. and Watts, C. (1995). Macropinocytosis. *Trends Cell Biol.* **5**, 424-428.

Urrutia, R., Henley, J. R., Cook, T. and McNiven, M. A. (1997). The dynamins: redundant or distinct functions for an expanding family of related GTPases? *Proc. Natl. Acad. Sci. USA* **94**, 377-384.

Yao, Q., Chen, J., Cao, H., Orth, J. D., McCaffery, J. M., Stan, R. V. and McNiven, M. A. (2005). Caveolin-1 interacts directly with dynamin-2. *J. Mol. Biol.* **348**, 491-501.

Zuchner, S., Noureddine, M., Kennerson, M., Verhoeven, K., Claeys, K., De Jonghe, P., Merory, J., Oliveira, S. A., Speer, M. C., Stenger, J. E. et al. (2005). Mutations in the pleckstrin homology domain of dynamin 2 cause dominant intermediate Charcot-Marie-Tooth disease. *Nat. Genet.* **37**, 289-294.